Journal of Geophysical Research: Space Physics

RESEARCH ARTICLE
10.1029/2018JA026081

The Transition Between Antiparallel and Component Magnetic Reconnection at Earth's Dayside Magnetopause

K. J. Trattner[1], J. L. Burch[2], P. A. Cassak[3], R. Ergun[1], S. Eriksson[1], S. A. Fuselier[2,4], B. L. Giles[5], R. G. Gomez[2], E. W. Grimes[6], S. M. Petrinec[7], J. M. Webster[8], and F. D. Wilder[1]

[1]LASP, University of Colorado Boulder, Boulder, CO, USA, [2]Southwest Research Institute, San Antonio, TX, USA, [3]Department of Physics and Astronomy, West Virginia University, Morgantown, WV, USA, [4]Department of Physics and Astronomy, University of Texas at San Antonio, San Antonio, TX, USA, [5]NASA/GSFC, Greenbelt, MD, USA, [6]Institute of Geophysics and Planetary Physics, Department of Earth and Space Sciences, UCLA, Los Angeles, CA, USA, [7]Lockheed-Martin ATC, Palo Alto, CA, USA, [8]Department of Physics and Astronomy, Rice University, Houston, TX, USA

Key Points:
- Antiparallel magnetic reconnection is dominant at the Earths magnetopause
- Antiparallel magnetic reconnection seems to control where component reconnection will occur

Correspondence to:
K. J. Trattner,
karlheinz.trattner@lasp.colorado.edu

Citation:
Trattner, K. J., Burch, J. L., Cassak, P. A., Ergun, R., Eriksson, S., Fuselier, S. A., et al (2018). The transition between antiparallel and component magnetic reconnection at Earth's dayside magnetopause. *Journal of Geophysical Research: Space Physics*, *123*, 10,177–10,188. https://doi.org/10.1029/2018JA026081

Received 10 SEP 2018
Accepted 10 NOV 2018
Accepted article online 16 NOV 2018
Published online 28 DEC 2018

Abstract Magnetic reconnection at Earth's magnetopause is usually described by two different scenarios, antiparallel and component reconnection. The Maximum Magnetic Shear model combines these two scenarios at specific connection points known as the *Knee* regions. Using a database of confirmed magnetopause reconnection locations observed during Phase 1a of the Magnetospheric Multiscale mission, a recent study showed that the model predicts the reconnection locations correctly within 2 Earth radii 80% of the time. The study also revealed and confirmed the existence of *anomalies*, that is, a specific set of conditions/parameters for which the observed reconnection locations are significantly different than the predicted locations. The first anomaly, described in an earlier study, occurs during the equinoxes for events with interplanetary magnetic field (IMF) clock angles around 120° and 240°. Another previously unknown anomaly was found for events observed around December that also occurs for the same IMF clock angle ranges as the first anomaly. Several of the anomalous December events were observed in the dawn sector Knee region and show that a combination of a large dipole tilt with an IMF clock angle of about 140° causes the magnetopause antiparallel reconnection region to line up along the draped IMF. That causes a deflection of the Knee points and the predicted reconnection location. These events demonstrate that magnetic reconnection at the Earth's dayside magnetopause preferentially occurs in the antiparallel locations and only occurs along component reconnection line segments when the draped IMF field lines at the magnetopause no longer contact an antiparallel reconnection region.

1. Introduction

NASA's Magnetospheric Multiscale Mission (MMS; Burch et al., 2016) was launched to understand the physics of the electron diffusion region (EDR), where a fundamental physical process known as magnetic reconnection is initiated. Within the relatively small EDR at Earth's magnetopause, electrons become demagnetized (similar to the demagnetization of ions at a larger spatial scale), which causes geomagnetic and interplanetary magnetic field (IMF) lines to effectively break and reconnect, changing the magnetic topology of the plasma environment.

Targeting and finding the small EDRs on the magnetopause surface is a challenging task even for four identical MMS satellites with an orbit that was designed to skim the dayside magnetopause and sample reconnection signatures, for example, accelerated, oppositely directed unidirectional ion beams in the boundary layer between two distinct plasma regions. Various models that predict the most likely location of the reconnection X-line based on a maximization of specific parameters at the magnetopause have been published. Parameters that are considered to have an influence on the reconnection location include maximum reconnection outflow speed, asymmetric reconnection outflow speed, the reconnection electric field, the magnetic field energy in the reconnecting components, the current density, maximizing the reconnecting components of the magnetospheric and the draped magnetic fields, and maximizing the magnetic shear across the dayside magnetopause (e.g., Alexeev et al., 1998; Borovsky, 2013; Hesse et al., 2013; Moore et al., 2002; Schreier et al., 2010; Swisdak & Drake, 2007; Teh & Sonnerup, 2008; Trattner et al., 2007).

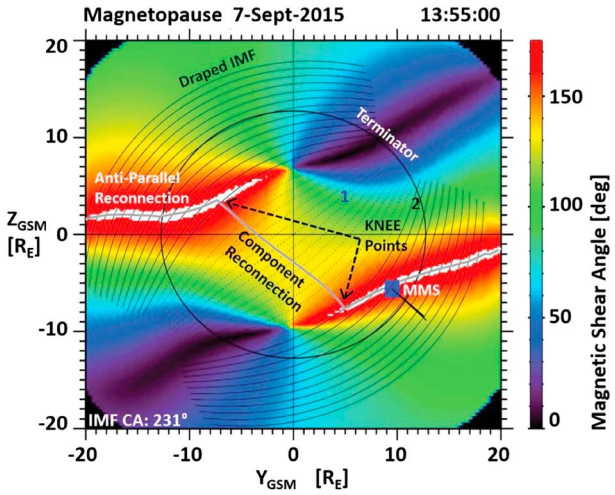

Figure 1. Magnetopause shear angle plot for an MMS magnetopause crossing on 7 September 2015 at 13:55 UT. The MMS satellites (blue symbols) are located in the southern dusk sector next to the antiparallel reconnection region. The gray line crossing the dayside magnetopause is the component reconnection tilted X-line, which connects to the antiparallel reconnection X-lines in the Knee points, as predicted by the Maximum Magnetic Shear model. Overlaid on the magnetic shear angle plot are some draped IMF lines that are used to determine the local magnetic shear at the magnetopause. MMS = Magnetospheric Multiscale; IMF = interplanetary magnetic field.

The empirical Maximum Magnetic Shear model (Trattner et al., 2007) predicts the dayside reconnection X-line to form at the ridge of maximum magnetic shear between the internal magnetospheric magnetic field and the external draped IMF. By extending across the entire dayside magnetopause, that model X-line is effectively a combination of the antiparallel reconnection scenario (e.g., Dungey, 1961; Luhmann et al., 1984) and the component tilted X-line scenario (e.g., Gonzalez & Mozer, 1974; Sonnerup, 1974; more details are provided in section 3 and Figure 1). The model also predicts that during IMF clock angles (arctan (B_Y/B_Z), where 0° is defined as pointing due north) within ±25° of a southward magnetic field or events occurring during a mainly radial magnetic field (IMF$|B_X|/B > 0.7$) the reconnection process reverts to an antiparallel reconnection scenario with no component reconnection tilted X-line present. Several magnetopause reconnection studies and MHD simulations have successfully used and confirmed the model predictions (e.g., Dunlop et al., 2011; Fuselier et al., 2011; Komar et al., 2015; Petrinec et al., 2011; Trattner et al., 2012, Trattner, Thresher, et al., 2017, Trattner, Burch, et al., 2017; Vines et al., 2017).

In a recent study to determine our ability to predict the location of the reconnection X-line at Earth's magnetopause, Trattner, Burch, et al. (2017) used the Maximum Magnetic Shear model together with 302 confirmed MMS X-line encounters and showed that the model predicts the location correctly (to within 2 R_E) in about 80% of the events. In addition, the study revealed anomalies, events where the MMS X-line encounters do not match the model prediction. However, these anomalies were not randomly distributed across the time window of the survey (Phase 1a of the MMS dayside magnetopause scan), which would indicate an issue with the assumptions in the model. The anomalous events concentrate onto very specific internal and external conditions, which led to the conclusion that something fundamentally changed across the dayside magnetopause causing a deflection of the reconnection locations.

For events observed around the equinoxes (no dipole tilt), the Maximum Magnetic Shear model predicts that the component reconnection tilted X-line segment should cross the dayside magnetopause in the vicinity or at the subsolar location, in agreement with the original component reconnection tilted X-line model (e.g., Gonzalez & Mozer, 1974; Sonnerup, 1974). These subsolar reconnection locations were indeed observed across the magnetopause (Trattner et al., 2007; Trattner, Burch, et al., 2017). However, for events with IMF clock angles around 120° and 240°, the measured X-line location shifted considerably either north or south of the subsolar region.

The second, previously unknown, anomaly observed in the MMS Phase 1a survey occurs for events observed around December (maximum dipole tilt). Curiously, these events shared the same IMF clock angle conditions as the equinox anomaly events. For symmetry reasons, we expect that a similar anomaly should also be present during the summer months. However, due to the MMS orbit apogee being located in the magnetotail during the summer months, such a mirror anomaly could not be confirmed.

A detailed analysis of the equinox anomaly is still in the planning phase. For this study we investigate the second, previously unknown, December anomaly. Due to the MMS orbit phase, many of the MMS magnetopause X-line encounters during this time occurred in the dawn sector close to local noon. With an IMF clock angle of about 120°, the MMS location along the extended dayside X-line location would fall into the transition region between the antiparallel and the component reconnection X-lines, the Knee region. Our investigation shows that the combination of a large dipole tilt with the IMF clock angles ranges mentioned above causes the magnetopause antiparallel region to line up along the draped IMF. This causes the Knee points and therefore the anchor point for the component reconnection tilted X-line crossing the dayside magnetopause to move to a different location. This investigation highlights the importance of antiparallel reconnection process that seem to be the preferred scenario and might even, through the location of the Knee points, control where component reconnection is occurring.

2. Data Selection, Instrumentation and Methodology

This study uses observations from the four MMS satellites (Burch et al., 2016), in particular the Fast Plasma Instrument (FPI; Pollock et al., 2016), the Fluxgate Magnetometer (FGM; Russell et al., 2016; Torbert et al., 2016), and the Hot Plasma Composition Analyzer (HPCA; Young et al., 2016).

The FPI instrument makes rapid phase space density measurements of electrons and ions. The instrument covers an energy range from 10 eV/e to 30 keV/*e* with a time resolution for ion measurements of 150 ms. In this study we use FPI ion spectrograms and velocity moments (survey mode) to identify magnetopause crossings and boundary layers in combination with observations from the FGM instrument to determine magnetic topology.

HPCA provides ion composition measurements in the energy range from 10 eV/e to 40 keV/*e* for the major magnetospheric ion species (H^+, He^{++}, He^+, and O^+). To achieve accurate measurements of the minor magnetopsheric ion species, the HPCA instrument employs a unique radio frequency (RF) unit in the ion optics independent of the time-of-flight section. The RF signal artificially reduces the proton flux at a range of energies from about 500 eV to 4 keV (in phase 1a). This RF signal reduces the proton contamination of minor ion species in areas where the proton flux is high. Details of this procedure are described in Burch et al. (2005) and Young et al. (2016).

Solar wind and IMF data used to determine the magnetic shear angle plots for the identified X-line encounters are available at CDAWeb. These solar wind context measurements are provided by the Wind Solar Wind Experiment (Ogilvie et al., 1995) and the Wind Magnetic Field Instrument (Lepping et al., 1995). To determine the correct solar wind convection times from the upstream satellite to the magnetopause, solar wind magnetic field rotations at the Wind satellite are individually lined up with magnetosheath magnetic field rotations observed by MMS/FGM. That ensures the most accurate magnetic shear angle plots and subsequently, through the Maximum Magnetic Shear model, the most accurate prediction of the location of the dayside X-line.

The procedure to determine the magnetopause shear angle plot is described in Trattner et al. (2007) and involves the internal T96 magnetic field model (Tsyganenko, 1995) together with the external analytic magnetic field draping model by Kobel and Flückiger (1994). The magnetic shear angle plots are used to determine the ridge of maximum magnetic shear across the dayside magnetopause, which defines the predicted location of the X-line that is subsequently compared with the observed X-line locations by MMS. These magnetospheric magnetic field and draping models are not perfect models of the magnetosphere and magnetosheath, respectively, yet they have been very successful tools for predicting the dayside reconnection location based upon estimates of the local magnetic shear angles. In addition, studies have shown the remarkable accuracy of the models with an average error between the observed and model magnetopause shear angles at the satellite location of only 13° (Trattner, Thresher, et al., 2017).

3. Observations

This study investigates one of the X-line location anomalies discovered in the Maximum Magnetic Shear model (e.g., Trattner et al., 2007) that was documented in a recent study with 302 magnetopause X-line locations observed by the MMS satellites during Phase 1a of the mission (Trattner, Burch, et al., 2017). As mentioned above, the Maximum Magnetic Shear model combines the two dominant reconnection scenarios, antiparallel (e.g., Crooker, 1979) and component magnetic reconnection (e.g., Sonnerup, 1974), creating a continuous dayside X-line, which follows the ridge of the maximum magnetic shear. Of particular interest along the long dayside X-line are the connection points (Knee points) between the component and antiparallel reconnection scenarios, which influences the location of the component reconnection line.

Figure 1 shows the magnetic shear angle plot for Earth's magnetopause on 7 September 2015 at 13:55 UT, as seen from the Sun. Red areas represent magnetopause regions with high magnetic shear, with embedded white areas representing the antiparallel reconnection regions within 3° of being exactly antiparallel. The gray line crossing the dayside magnetopause represents the predicted extended X-line, which consists of two segments in the antiparallel reconnection regions, located in the northern dawn and southern dusk sectors, connected by a component reconnection tilted X-line at the Knee points. The MMS satellites (blue symbol) are located in the magnetopause boundary layer in the southern dusk sector close to where the

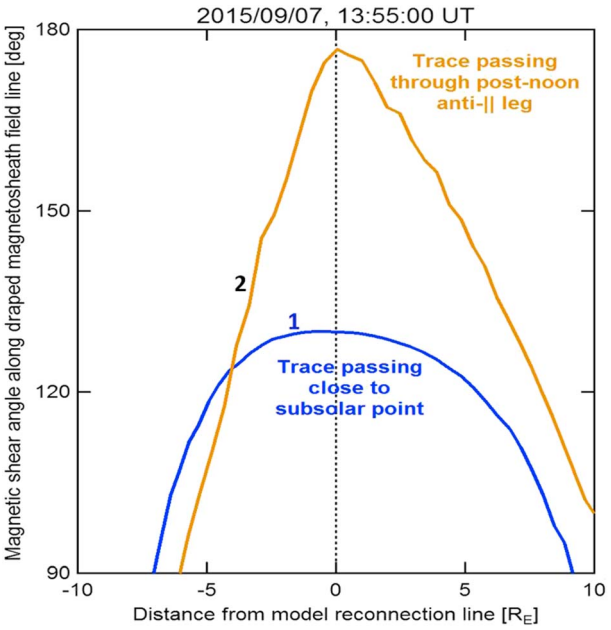

Figure 2. The magnetic shear angle along two draped interplanetary magnetic field lines, which cross the subsolar region and the antiparallel reconnection region (as marked in Figure 1), with respect to the location of the predicted X-line at the magnetopause.

terminator plane (T; X_{GSM} = 0) intersects the magnetopause. The MMS satellites are also close to the predicted X-line in the antiparallel reconnection region and observe strong southward-eastward ion jets from the reconnection region just north of the satellite location. These jets are depicted in Figure 1 as black lines emanating from the MMS symbol and represent the FPI bulk velocity flow vectors in the *Y-Z* GSM projection.

Overlaid on the magnetic shear angle plot in Figure 1 are some of the draped IMF lines from the Kobel and Flückiger (1994) model that are used to create the magnetic shear angle plot. The local magnetic shear along these draped IMF lines is maximized to determine the location of the X-line across the magnetopause. Two of the draped IMF lines, (1) crossing the subsolar region and (2) crossing the antiparallel reconnection region in the southern dusk sector, have been labeled to demonstrate the methodology.

Figure 2 shows the magnetic shear along the IMF lines (1) and (2), centered on the location of the predicted X-line from the Maximum Magnetic Shear model. The magnetic shear profile along the IMF line (2) shows a very sharp rise to a maximum of about 180° as it crosses the antiparallel reconnection region. Note that the procedure to create that plot uses a line across a magnetic shear angle, both of which are discretized and therefore introduce small errors, so small deviations from the ideal 180° magnetic shear are to be expected. For IMF lines crossing the antiparallel reconnection region, the identification of the maximum magnetic shear location along these draped field lines is generally easy. In contrast, IMF line (1) crosses the dayside in the subsolar region and exhibit a flat, saddle-like plateau with a maximum magnetic shear of about 130°. The shape of the saddle region in the subsolar region was investigated by Petrinec et al. (2014) who showed that within 2 R_E of the predicted X-line location, the magnetic shear changes by less than 2°. Based on this result and considering that the models involved in the calculation of the magnetic shear across the magnetopause are not ideal either, the X-line location uncertainty was set to 2 R_E.

Figure 3 shows the distance of the 302 MMS X-line encounters observed during Phase 1a (Trattner, Burch, et al., 2017) from the predicted reconnection location versus the IMF clock angles of the events. While 80% of the events are within the model uncertainty of 2 R_E (dotted line), the IMF clock angles around 120° and 240° showed larger errors and are associated with the fall and spring equinoxes, respectively. The previously unknown December anomaly first showed up for MMS X-line locations close to the Knee points at the magnetopause (see Figure 1 and green symbols in Figure 3). In the original study, 11 of the 302 events show this particular location anomaly. In the recent months, four additional events were identified that also fall into this category. It should be noted that the X-line location anomalies do not occur exactly for the IMF clock angles mentioned above since daily variations of the Earth's dipole tilt as well as the presence of a variable IMF B_X component cause changes for the magnetopause magnetic shear and therefore create a clock angle range for the occurrence of the anomaly.

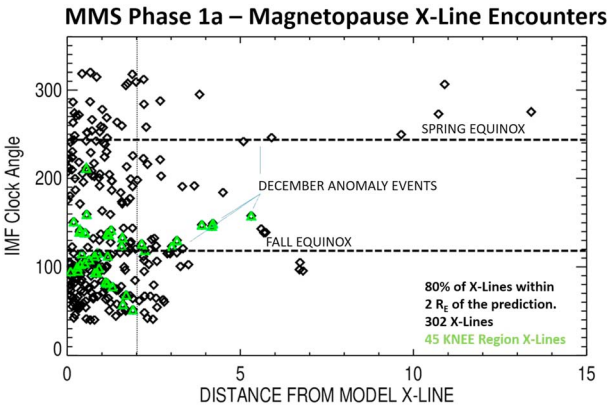

Figure 3. The distance between the locations of 302 MMS X-line encounters from the predicted Maximum Magnetic Shear model reconnection line versus the IMF clock angle. The anomalies occur for IMF clock angles around 120° and 240°. MMS X-line encounters observed in the Knee regions are marked with green symbols. MMS = Magnetospheric Multiscale; IMF = interplanetary magnetic field.

One of the anomalous Knee events with multiple X-line crossings was observed by MMS on 14 December 2015, between 01:00 to 02:00 UT. The panels in Figure 4 show data from the MMS3 satellite and contain from top to bottom the FPI ion energy spectrogram (keV/cm^2 sr s keV), the FGM magnetic field components (nT) in GSM, the FGM magnetic field magnitude (nT), the FPI density (cm^{-3}), and the FPI ion velocity moments (km/s). As designed in the MMS mission profile, the MMS3 satellite skimmed along the magnetopause and crossed the magnetopause multiple times, observing accelerated ion beams in the magnetopause

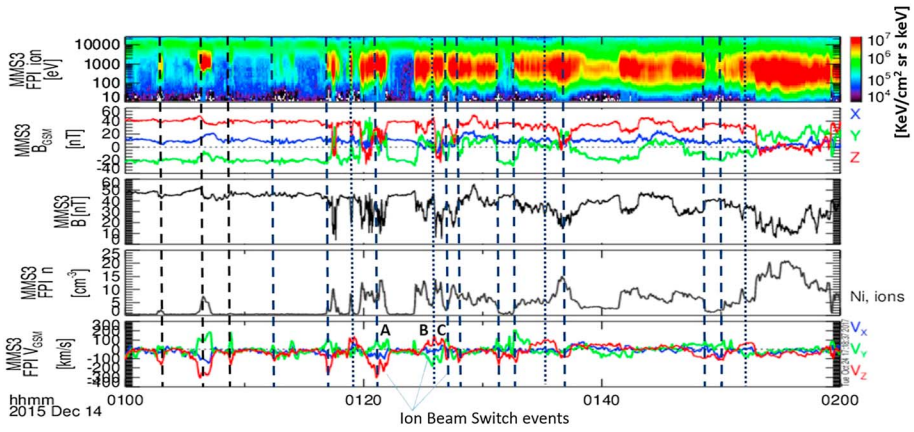

Figure 4. MMS3 magnetopause crossings on 14 December 2015 showing several switching ion beams in the magnetopause boundary layer. Plotted from top to bottom are the FPI energy flux spectrogram (keV/(cm^2 s sr keV)), the FGM magnetic field components in GSM (nT), the FGM magnetic field magnitude (nT), the FPI plasma density (cm^{-3}), and the FPI plasma velocity moments (km/s) in GSM coordinates. FPI = Fast Plasma Instrument; FGM = Fluxgate Magnetometer.

boundary layers that indicate the presence of an active reconnection site. In Figure 4, southward and northward directed ion beams are marked with dashed and dotted lines, respectively. Switching ion beam directions in the magnetopause boundary layers are a well-known signature and are used to identify magnetopause reconnection locations (e.g., Cowley, 1982; Dunlop et al., 2011; Gosling et al., 1982; Paschmann et al., 1979; Pu et al., 2007; Trenchi et al., 2008).

Between 01:00 to 02:00 UT on 14 December 2015, MMS observed 17 individual ion beams with 7 distinctive switches of the ion beam direction. The spacecraft remained very near a reconnection site and, in fact, passed through an EDR at 01:17.30 UT (e.g., Webster et al., 2018). Details about this EDR encounter can be found in several publications (e.g., Chen et al., 2017; Ergun et al., 2017; Graham et al., 2017).

MMS3 observes the second ion beam switch at 01:20.59 UT (A) (shortly after the diffusion region encounter) where a northward ion beam from a previous encounter with the magnetopause boundary layer is followed by a strong southward ion beam. The magnetopause encounter at 01:25.49 UT (B) shows again a northward ion beam followed by a southward ion beam at 01:26.59 UT (C).

Figure 5 shows HPCA proton distributions observed at all four MMS satellites for the respective times of the three ion beam observations mentioned above. The proton observations are plotted in field-aligned coordinates with the perpendicular bulk velocity removed. The ambient magnetic field direction in the panels is along the *Y* axis. For all three observation times the MMS satellites are located on northward magnetic fields in the low-latitude boundary layer of the magnetosphere. The top row in Figure 5 shows the proton distributions observed at (A). All MMS satellites observe D-shaped ion distributions moving antiparallel to the magnetic field. This streaming direction indicates an X-line located north of the satellite location. The center row in Figure 5 shows D-shaped proton distributions observed at (B), streaming parallel to the magnetic field, and emanating from an X-line south of the satellite locations. At (C), all distributions have changed again to a southward ion beam moving anti-parallel to the magnetic field. These repeated switches in the ion beam direction throughout the time interval and the presence of an EDR (e.g., Webster et al., 2018) are strong indications of a stable magnetopause X-line location at the position of the satellites.

Figure 6 shows two magnetic shear angle plots for (A) and (B) as defined in Figure 4. The format is the same as for Figure 1. In contrast to the example shown in Figure 1, the antiparallel reconnection regions are no longer clearly separated in different hemispheres. Due to the large dipole tilt in December combined with an IMF clock angle of 148°, the dawnside antiparallel reconnection region is close to the GSM $Z = 0$ equatorial plane before turning towards the southern cusp forming a hook-like shape. This creates unique magnetopause conditions where the draped IMF lines begin to line up along the antiparallel reconnection region.

The location of the MMS satellites in Figure 6 are again marked with blue symbols in between the antiparallel reconnection region and the GSM equatorial plane. Figure 6a shows a strong southward ion beam, while

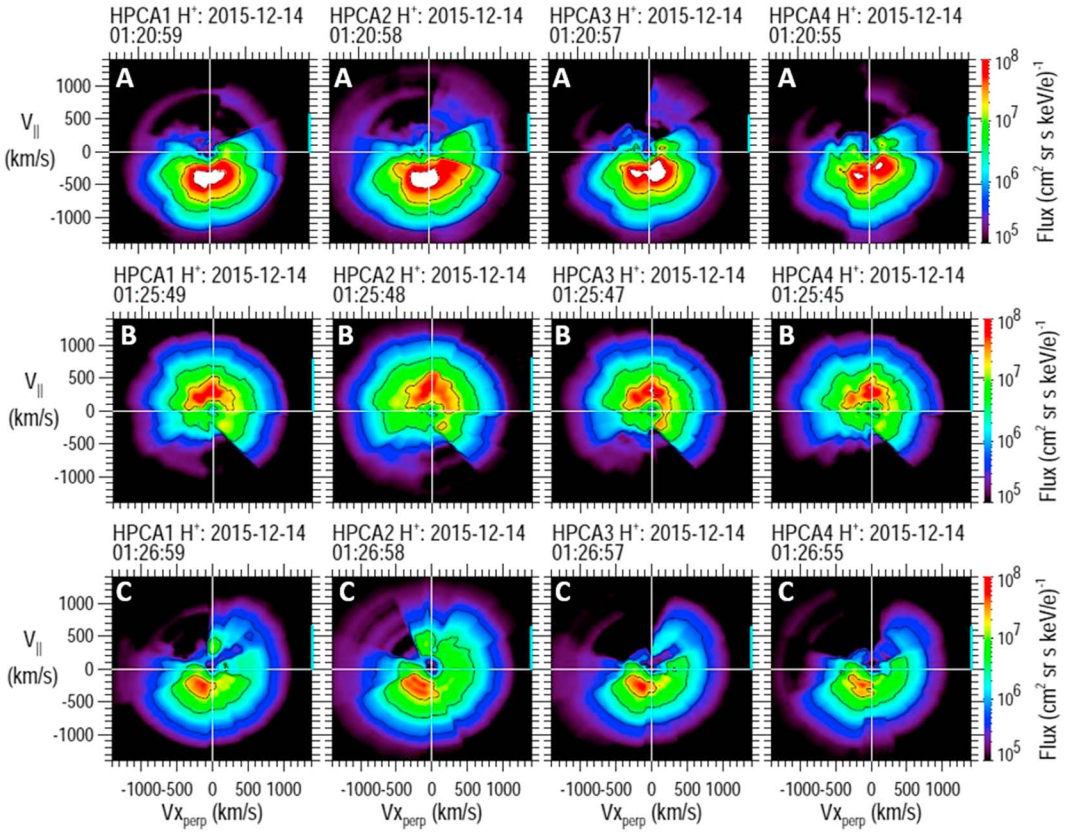

Figure 5. HPCA H^+ proton distributions from all 4 MMS satellites for three time periods marked in Figure 4. The distributions are plotted in field-aligned coordinates with the perpendicular bulk velocity removed and ion beam directions switching back and forth. HPCA = Hot Plasma Composition Analyzer; MMS = Magnetospheric Multiscale.

Figure 6b shows a northward beam at the location of the MMS satellites, confirming the presence of an X-line at that location. The MMS satellites encountered the X-line with the associated EDR about 4 minutes earlier at 01:17.30 UT as discussed in Chen et al. (2017) who reported a local guide field for that X-line encounter of about 0.2. This observed guide field translates into a local magnetic shear angle of about 158°. The local model magnetic shear angle at the MMS location as shown in Figure 6 for the time of the EDR encounter was 161°, well within the previously published uncertainty between the observed and model magnetopause shear angles at the satellite location of only 13° (e.g., Trattner, Thresher, et al., 2017). However, the predicted X-line location at the ridge of maximum magnetic shear across the dayside magnetopause is located more than 4 R_E north of the MMS location and clearly outside the usual uncertainty for the prediction model.

The left panel of Figure 7 shows the magnetic shear angle plot for (C) as defined in Figure 4, together with a line plot of the magnetic shear angle along two draped IMF lines (right panel), crossing the subsolar region (1) and close to the dawn anti-parallel reconnection region (2). The magnetic shear angle along the IMF line (1) has the typical flat maximum and resembles closely the magnetic shear angle profile shown in Figure 2. However, the situation is markedly different for the IMF line (2). The specific internal (dipole) and external (IMF clock angle of 147°) conditions cause the antiparallel reconnection region to line up along the draped IMF. Following the magnetic shear angle along the IMF line (2) now shows an extremely flat plateau for about 10 R_E, which greatly increases the difficulty to define a meaningful maximum magnetic shear location to define the position of the X-line. The observations showed that the actual X-line location is about 4 R_E away and its position is marked by a star along the magnetic shear angle line. While there appears to be a local maximum at that location, it should be noted that the algorithm to determine the maximum magnetic shear location applies a smoothing routine to avoid the X-line widely jumping around due to local spikes along the magnetopause surface, especially for sections when the maximum magnetic shear ridge becomes very flat.

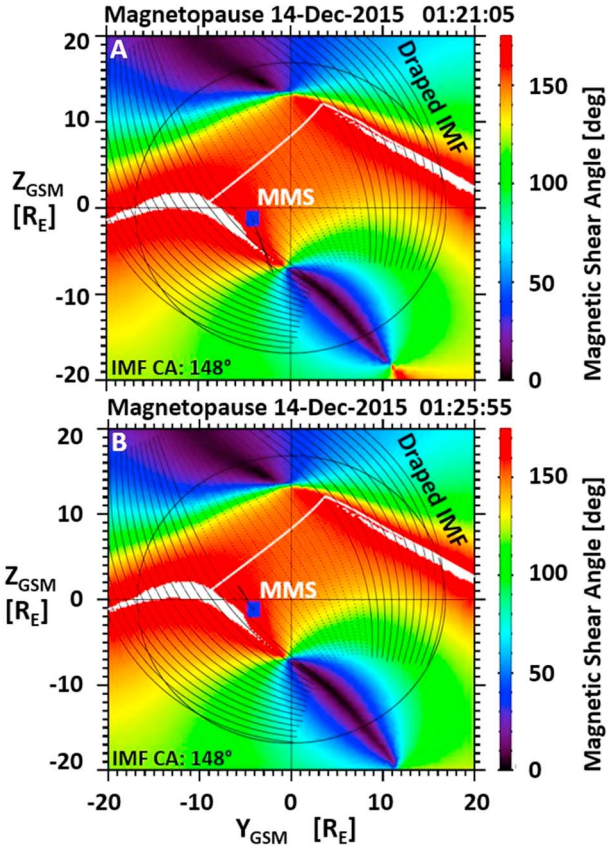

Figure 6. Two magnetopause magnetic shear angle plots for MMS boundary layer crossings on 14 December 2015 at 01:21.05 UT (upper panel) and 01:25.55 UT (lower panel). The blue symbol represents the location of the MMS satellites at the magnetopause showing a southward (a) and a northward ion beam (b), indicating the presence of an X-line more than 4 R_E away from the predicted X-line location. MMS = Magnetospheric Multiscale; IMF = interplanetary magnetic field.

The solution for this anomaly problem becomes apparent in the magnetic shear angle plot in the left panel of Figure 7. The location of the maximum magnetic shear X-line usually starts along a draped IMF line across the magnetopause intersecting the subsolar region and extends from there outward. Under these specific internal and external conditions, the determination of the maximum magnetic shear angle encounters a problem as it approaches the antiparallel reconnection region and the extended plateau region. However, Figure 7 shows that following the maximum magnetic shear angle beginning in the antiparallel region leads to a different result. The locations of the maximum magnetic shear angle along the IMF lines are marked with black dots in Figure 7 (left panel). For individual draped IMF lines the maximum magnetic shear angle location now follows the curved (hooked) antiparallel reconnection region toward the southern cusp region until we reach the first draped IMF line that does not cross the antiparallel reconnection region (white area in Figure 7). That first draped IMF line that misses this region has a point that is closest to the antiparallel reconnection region also marked with a black dot along the draped IMF line. And this location is also the location where the MMS satellites observed seven consecutive ion beam switches and an EDR for the 14 December 2015, magnetopause encounter. This *closest approach* point for a draped IMF line is the location of the actual Knee point, the transition from the antiparallel reconnection X-line to the component reconnection tilted X-line. In Figure 7 (left panel) the black dots along the draped IMF lines turn gray and return to the original predicted component reconnection tilted X-line as it crosses the dayside magnetopause. However, this behavior of the X-line has not yet been confirmed.

Another event with an anomalous prediction of the magnetopause X-line location occurred on 17 January 2016 and is shown in Figure 8. The layout of the Figure is the same as in Figure 4. Between 06:25 and 06:42 UT during this magnetopause crossing, the MMS 3 satellite encountered nine accelerated ion beams during multiple boundary layer encounters which also contained four switches of the ion beam direction. The final

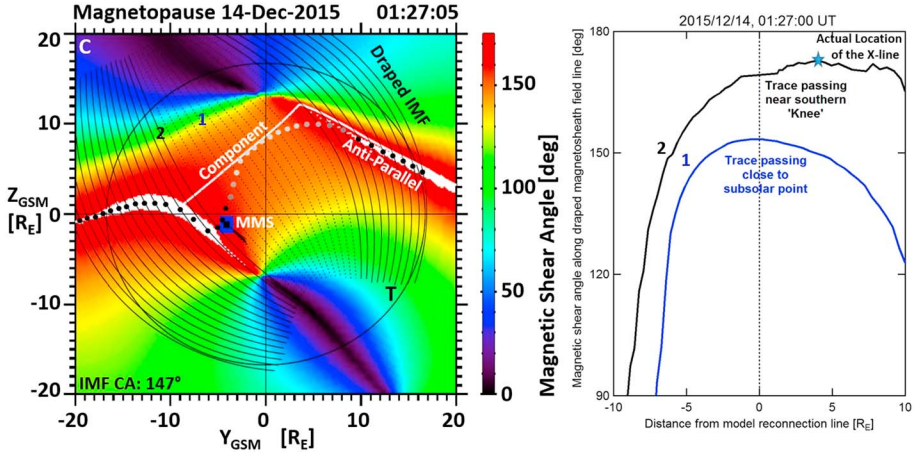

Figure 7. A magnetopause magnetic shear angle plot (left panel) and the magnetic shear along two draped IMF lines at the magnetopause (right panel) as marked in the shear angle plot. The draped IMF lines in the dawn sector line up along the antiparallel reconnection region, which causes an unusual flat plateau for the magnetic shear along the draped IMF line. The result is a deflection of the Knee point towards the southern cusp region and subsequently a deflection of the X-line location to the south. IMF = interplanetary magnetic field.

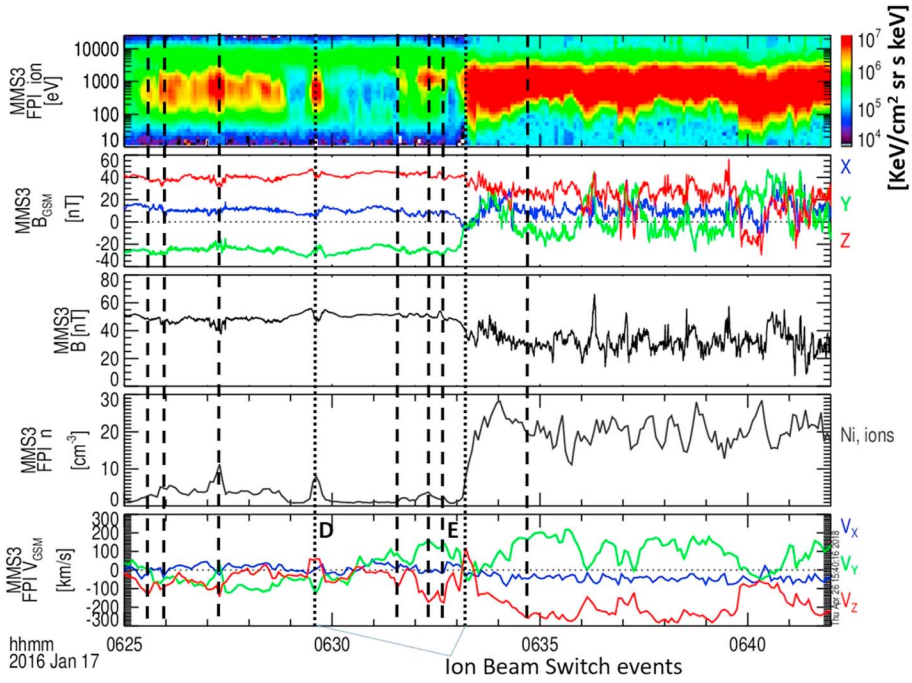

Figure 8. MMS3 magnetopause crossings on 17 January 2016 showing several switching ion beams in the magnetopause boundary layer. The format of the figure is the same as in Figure 4. FPI = Fast Plasma Instrument.

magnetopause crossing for the MMS satellites before crossing completely into the magnetosphere occurred at about 06:33 UT for which two of the ion beam switches occurred.

The two earlier ion beam switches were observed at 06:29.40 UT (D) and 06:32.10 UT (E) and are shown in Figure 9. The magnetic shear angle plots shown in Figure 9 have the same layout as Figure 6. As with the previous example, the antiparallel reconnection region in the dawn sector is again located along the GSM equator plane before turning toward the southern cusp, creating a hook and lining up along the draped IMF direction. The left panel of Figure 9 shows the magnetopause conditions at (D) during an IMF clock angle of about 120°. The MMS3 satellite is located about 3 R_E south of the predicted X-line and observed a northward ion beam which can only come from an X-line south of the satellite. The right panel of Figure 9 shows the conditions at (E) during an IMF clock angle of 125° when MMS3 observed a southward ion beam.

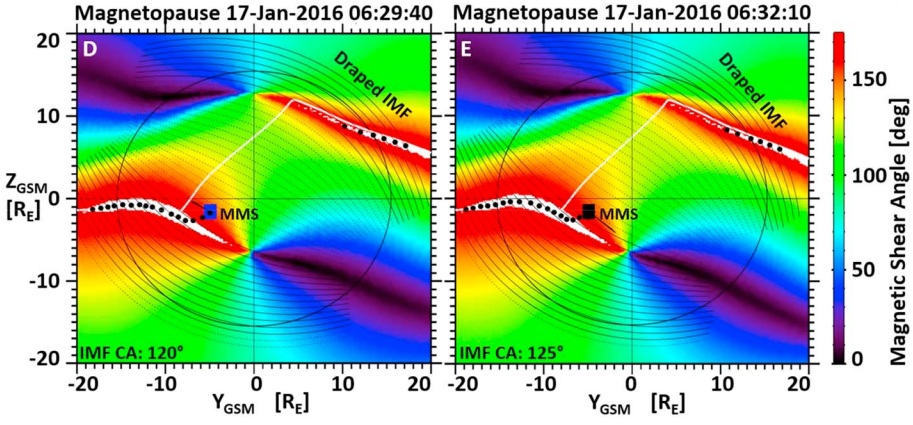

Figure 9. The magnetopause shear angle plots for the MMS magnetopause crossing during one of the ion beam switches on 17 January 2016 at 06:29.40 UT (left panel) and 06:32.10 UT (right panel). The MMS locations at the magnetopause, marked by blue symbols, are far away from the predicted reconnection location but match the deflected location of the knee points (last draped IMF line still crossing into the antiparallel reconnection region). MMS = Magnetospheric Multiscale; IMF = interplanetary magnetic field.

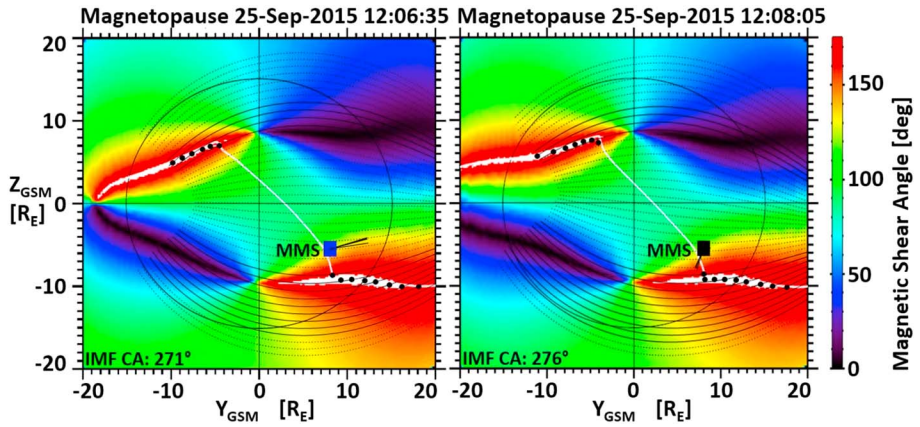

Figure 10. The magnetopause shear angle plots for the MMS magnetopause crossing during the ion beam switch on 25 September 2015 at 12:06.35 UT (left panel) and 12:08.05 UT (right panel). The MMS locations at the magnetopause, marked by blue and black symbols, are a very good match for the predicted location of the X-line. That location also matches the knee points (i.e., the last draped IMF line intersecting the antiparallel reconnection region).
MMS = Magnetospheric Multiscale; IMF = interplanetary magnetic field.

Marking again the maximum shear angle location along the draped IMF with black dots and starting in the antiparallel reconnection region, the X-line follows the hooked shape towards the southern cusp until the draped IMF field line no longer intercepts the antiparallel reconnection region. That defines the Knee point and coincides with the location of the MMS satellites and the observed ion beam switches.

As long as draped IMF lines have access to the antiparallel reconnection site, this is where magnetic reconnection will occur. The component reconnection tilted X-line in the magnetic shear angle plots of Figure 9 has not been completed across the magnetopause to the other antiparallel reconnection region in the dusk sector since it is currently unclear which of the following possibilities is dominating. As indicated in Figure 7, the X-line could return the maximum shear angle location and then agree with the original definition of the Maximum Magnetic Shear model. However, it is also possible that the component reconnection tilted X-line simply connects between the new Knee points and runs considerably south of the currently predicted X-line. That would mean that antiparallel reconnection not only is the dominant reconnection scenario but also controls the location of the component reconnection line.

As discussed above, the Maximum Magnetic Shear model does predict the location of the X-line correctly in 80% of the investigated cases. Considering the present result about the apparent importance of the draped IMF interacting with the antiparallel reconnection region to define the position of the Knee points and subsequently the location of the component reconnection X-line, we have spot checked events in the original study where the location of the X-line was predicted correctly. Figure 10 shows the magnetic shear angle plots for such a successfully predicted ion beam switch event, observed during the MMS magnetopause crossing on 25 September 2015. The layout of Figure 10 is the same as in Figure 6. The events occurred for IMF clock angles of about 273° and show the antiparallel reconnection regions clearly separated in different hemispheres. The MMS satellites, located in the southern dusk sector at the predicted X-line location, observed northward beams in the MSBL at 12:06.35 UT (left panel) and southward ion beams in the low-latitude boundary layer at 12:08.05 UT. In addition, the subsequent analysis of this beam switch event using the Webster et al. (2018) methodology revealed the presence of a previously unknown EDR at 12:07.03 UT. The overlay of the draped IMF lines reveals that the location of the predicted Knee points are in agreement with the location of the closest approach for the first draped IMF lines that no longer cross the antiparallel reconnection region. The Maximum Magnetic Shear model appears to have the conditions for selecting Knee points at that location automatically built in and only fails under extreme dipole tilts with specific IMF clock angles that cause the antiparallel reconnection region to line up along the draped IMF.

4. Summary and Conclusions

In a recent study by Trattner, Burch, et al. (2017), predictions of the dayside magnetopause reconnection locations by the Maximum Magnetic Shear model were tested against an MMS database of confirmed

encounters with the reconnection location during Phase 1a. The model showed an accuracy of 80% to predict the dayside reconnection region within the 2 R_E model uncertainty, in agreement with earlier smaller studies (e.g., Fuselier et al., 2011, Dunlop et al., 2011; Petrinec et al., 2011; Trattner et al., 2012; Vines et al., 2017). The study also revealed two major anomalies in the ability to predict the dayside reconnection location, (1) for events observed around the equinoxes (no dipole tilt) and (2) for events around December (maximum dipole tilt). In addition to this internal parameter, both anomalies share also an external parameter, the IMF clock angle. For the equinox anomaly events the IMF clock angle is either around 120° or 240° for the spring and fall equinoxes, respectively. For December anomaly events, both of these IMF clock angles have been observed. It was concluded that these internal and external parameter ranges are so specific that there must be a fundamental change of the conditions at the magnetopause causing these alternative reconnection locations. This study is a follow-up of the Trattner, Burch, et al. (2017) study where these anomalies are documented, and investigates the December anomaly events.

The Maximum Magnetic Shear model (Trattner et al., 2007) combines the traditional antiparallel reconnection scenario (e.g., Dungey, 1961; Luhmann et al., 1984) with the component reconnection tilted X-line scenario (e.g., Gonzalez & Mozer, 1974; Sonnerup, 1974) and predicts long uninterrupted X-lines crossing the dayside magnetopause along the ridge where the magnetic shear is a maximum. For IMF clock angles within ±25° of a southward field or large IMF B_X components ($|B_X|/B > 0.7$) the model predicts reconnection in the antiparallel reconnection region and no component reconnection tilted X-line.

The antiparallel reconnection regions at Earth's magnetopause are usually located in opposing hemispheres in the dawn and dusk sectors. The analysis of the December anomaly events showed that for a large dipole tilt together with IMF clock angles around 120°, the antiparallel reconnection region in the dawn sector is close to the GSM $Z = 0$ equator before turning towards the cusp regions. For these conditions, the draped IMF begins lining up along the antiparallel reconnection region causing the deflection of the Knee point, the transition between the antiparallel and component reconnection segments, and subsequently the reconnection location of the component reconnection line.

The analysis of the December anomaly events showed that magnetic reconnection is present in the antiparallel reconnection region as long as draped IMF lines at the magnetopause cross it. The Knee points are located where the first draped IMF line that did not cross the antiparallel reconnection region has its closest approach to that region. Spot checking other magnetopause X-line encounters from the Phase 1a survey where the model prediction was correct reveals that this condition is the default solution for the Maximum Magnetic Shear model, which confirms the current high prediction accuracy. Only under specific internal and external conditions, for example, the IMF draping along the antiparallel reconnection region, a deflection of the Knee points is observed. That deflection was not previously considered in the model and will be included in future studies. Reconnection events in the summer months should have a similar anomaly point for symmetry reasons, thought this cannot be tested with MMS because during these months the satellites are in the magnetotail.

It should be noted that magnetopause reconnection events observed during large dipole tilt conditions are also known to cause multiple magnetopause reconnection lines (Fuselier et al., 2018; Hasegawa et al., 2010; Trenchi et al., 2011). This scenario was predicted in simulations (e.g., Raeder, 2006) that reported on the existence of a secondary X-line passing roughly through the subsolar point, while the main X-line appeared along the location of the magnetic equator. Multiple X-lines at the magnetopause (e.g., Lee & Fu, 1985) are generally known as a source for flux transfer events (FTEs), a transient phenomenon, which are not part of this study. FTEs have been carefully excluded from the database (Trattner, Burch, et al., 2017) using the appearance of bipolar magnetic field signatures and the existence of multiple ion beams in the magnetopause boundary layers. In contrast to multiple ion distributions in the boundary layers (e.g., Fuselier et al., 2018), pointing to the temporary existence of a secondary X-line at the magnetopause, the events discussed in this study only show single D-shaped distributions which switch directions when MMS crosses the X-line.

Antiparallel magnetic reconnection appears to be the dominant reconnection process at Earth's magnetopause, defining where the transition points to the component reconnection line are located. For the events that show a deflection of the Knee location, it is currently unclear if the component reconnection tilted X-line returns to the predicted maximum magnetic shear location across the dayside magnetopause or if the deflected Knee points are directly connected by a magnetic reconnection X-line. The latter would mean

that antiparallel magnetic reconnection not only is the dominant preferred reconnection scenario at Earth's magnetopause but also controls and defines where component magnetic reconnection can happen. A MMS event survey is forthcoming to identify X-line encounters in the subsolar regions for dipole and IMF draping conditions that cause the deflection of the Knee points to confirm the fate of the component reconnection X-line.

The dominance of the antiparallel reconnection process might also explain a long-standing problem, the ±25° cutoff angle around the true southward IMF direction reported in the original study that led to the development of the Maximum Magnetic Shear model (Trattner et al., 2007). For these events, a component reconnection tilted X-line no longer exists. The solution could be that all draped IMF lines have access to the antiparallel reconnection region and the presence of two cusps define the observed exclusion angle. A MMS event search for X-line locations close to local noon during strong southward IMF conditions is considered to test this idea.

Another interesting situation might arise for a case where the draped IMF line perfectly lines up with the antiparallel reconnection region and not truly crosses it. Instead of the relative sharply defined X-line at the point of highest magnetic shear, the region where the fields are antiparallel could be several Earth radii long, which should produce an unusual diffusion region.

Acknowledgments
Solar wind observations were provided by the Wind *Solar Wind Experiment* (Wind/SWE; Ogilvie et al., 1995). The IMF measurements are provided by the Wind *Magnetic Field Instrument* (Wind/MFI; Lepping et al., 1995). The solar wind data are available at CDAWeb (http://cdaweb.gsfc.nasa.gov/istp_public/). All data from the first 6 months of the MMS mission are available to the general public through the MMS website. The research at LASP is supported by NASA grant NNX14AF71G. Research at SWRI was funded by NASA grant NNX11AF71G. Research at Lockheed Martin was funded by NASA contract 499935Q.

References

Alexeev, I. I., Sibeck, D. G., & Bobrovnikov, S. Y. (1998). Concerning the location of magnetopause merging as a function of the magnetopause current strength. *Journal of Geophysical Research*, *103*(A4), 6675–6684.

Borovsky, J. E. (2013). Physical improvements to the solar wind reconnection control function for the Earth's magnetosphere. *Journal of Geophysical Research: Space Physics*, *118*, 2113–2121. https://doi.org/10.1002/jgra.50110

Burch, J. L., Miller, G. P., De Los Santos, A., Pollock, C. J., Pope, S. E., Valek, P. W., & Young, D. T. (2005). Technique for increasing the dynamic range of space-borne ion composition instruments. *The Review of Scientific Instruments*, *76*, 103301.

Burch, J. L., Moore, T. E., Torbert, R. B., & Giles, B. L. (2016). Magnetospheric multiscale overview and science objectives. *Space Science Reviews*, *199*(1-4), 5–21. https://doi.org/10.1007/s11214-015-0164-9

Chen, L.-J., Hesse, M., Wang, S., Gershman, D., Ergun, R. E., Burch, J., et al. (2017). Electron diffusion region during magnetopause reconnection with an intermediate guide field: Magnetospheric multiscale observations. *Journal of Geophysical Research: Space Physics*, *122*, 5235–5246. https://doi.org/10.1002/2017JA024004

Cowley, S. W. H. (1982). The cause of convection in the Earth's magnetosphere: A review of developments during the IMS. *Reviews of Geophysics and Space Physics*, *20*, 531–565.

Crooker, N. U. (1979). Dayside merging and cusp geometry. *Journal of Geophysical Research*, *84*, 951–959.

Dungey, J. W. (1961). Interplanetary magnetic field and auroral zones. *Physical Review Letters*, *6*, 47–48.

Dunlop, M. W., Zhang, Q.-H., Bogdanova, Y. V., Trattner, K. J., Pu, Z., Hasegawa, H., et al. (2011). Magnetopause reconnection across wide local time. *Annales de Geophysique*, *29*, 1683–1697.

Ergun, R. E., Chen, L. J., Wilder, F. D., Ahmadi, N., Eriksson, S., Usanova, M. E., et al. (2017). Drift waves, intense parallel electric fields, and turbulence associated with asymmetric magnetic reconnection at the magnetopause. *Geophysical Research Letters*, *44*, 2978–2986. https://doi.org/10.1002/2016GL072493

Fuselier, S. A., Petrinec, S. M., Trattner, K. J., Broll, J., Burch, J. L., Giles, B. L., et al. (2018). Observational evidence of large-scale multiple reconnection at the Earth's dayside magnetopause. *Journal of Geophysical Research: Space Physics*, *123*, 8407–8421. https://doi.org/10.1029/2018JA025681

Fuselier, S. A., Trattner, K. J., & Petrinec, S. M. (2011). Anti-parallel and component reconnection at the dayside magnetopause. *Journal of Geophysical Research*, *116*, A10227. https://doi.org/10.1029/2011JA016888

Gonzalez, W. D., & Mozer, F. S. (1974). A quantitative model for the potential resulting from reconnection with an arbitrary interplanetary magnetic field. *Journal of Geophysical Research*, *79*, 4186–4194.

Gosling, J. T., Asbridge, J. R., Bame, S. J., Feldman, W. C., Paschmann, G., Sckopke, N., & Russell, C. T. (1982). Evidence for quasi stationary reconnection at the dayside magnetopause. *Journal of Geophysical Research*, *87*, 2147.

Graham, D. B., Khotyaintsev, Y. V., Vaivads, A., Norgren, C., André, M., Webster, J. M., et al. (2017). Instability of agyrotropic electron beams near the electron diffusion region. *Physical Review Letters*, *119*, 025101.

Hasegawa, H., Wang, J., Dunlop, M. W., Pu, Z. Y., Zhang, Q. H., Lavraud, B., et al. (2010). Evidence for a flux transfer event generated by multiple X-line reconnection at the magnetopause. *Geophysical Research Letters*, *37*, L16101. https://doi.org/10.1029/2010GL044219

Hesse, M., Aunai, N., Zenitani, S., Kuznetsova, M., & Birn, J. (2013). Aspects of collisionless magnetic reconnection in asymmetric systems. *Physics of Plasmas*, *20*(6), 061210.

Kobel, E., & Flückiger, E. O. (1994). A model of the steady state magnetic field in the magnetosheath. *Journal of Geophysical Research*, *99*, 23,617–23,622.

Komar, C. M., Fermo, R. L., & Cassak, P. A. (2015). Comparative analysis of dayside magnetic reconnection models in global magnetosphere simulations. *Journal of Geophysical Research: Space Physics*, *120*, 276–294. https://doi.org/10.1002/2014JA020587

Lee, L. C., & Fu, Z. F. (1985). A theory of magnetic flux transfer at the Earth's magnetopause. *Geophysical Research Letters*, *12*, 105–108.

Lepping, R. P., Schatfen, K. H., Mariani, E., Ness, N. E., Neubauer, E. M., Whang, Y. C., et al. (1995). The Wind magnetic field investigation. In C. T. Russell (Ed.), *The Global Geospace Mission* (pp. 207–227). The Netherlands: Kluwer Academic Press.

Luhmann, J. R., Walker, R. J., Russell, C. T., Crooker, N. U., Spreiter, J. R., & Stahara, S. S. (1984). Patterns of potential magnetic field merging sites on the dayside magnetopause. *Journal of Geophysical Research*, *89*, 1739–1742.

Moore, T. E., Fok, M.-C., & Chandler, M. O. (2002). The dayside reconnection X-line. *Journal of Geophysical Research*, *107*(A10), 1332. https://doi.org/10.1029/2002JA009381

Ogilvie, K. W., Chornay, D. J., Fritzenreiter, R. J., Hunsaker, F., Keller, J., Lobell, J., et al. (1995). SWE: A comprehensive plasma instrument for the Wind spacecraft. In C. T. Russell (Ed.), *The global geospace m*, (pp. 55–77). Norwell, Mass: Kluwer Academic Press.

Paschmann, G., Sonnerup, B. U. Ö., Papamastorakis, I., Sckopke, N., Haerendel, G., Bame, S. J., et al. (1979). Plasma acceleration at the Earth's magnetopause: Evidence for magnetic field reconnection. *Nature*, *282*, 243.

Petrinec, S. M., Dayeh, M. A., Funsten, H. O., Fuselier, S. A., Heirtzler, D., Janzen, P., et al. (2011). Neutral atom imaging of the magnetospheric cusp. *Journal of Geophysical Research*, *116*, A07203. https://doi.org/10.1029/2010JA016357

Petrinec, S. M., Trattner, K. J., Fuselier, S. A., & Stovall, J. (2014). The steepness of the magnetic shear angle 'saddle': A parameter for constraining the location of dayside magnetic reconnection? *Journal of Geophysical Research: Space Physics*, *119*, 8404–8414. https://doi.org/10.1002/2014JA020209

Pollock, C., Moore, T., Jacques, A., Burch, J., Gliese, U., Saito, Y., et al. (2016). Fast plasma investigation for Magnetospheric multiscale. *Space Science Reviews*, *199*(1-4), 331–406. https://doi.org/10.1007/s11214-016-0245-4

Pu, Z.-Y., Zhang, X. G., Wang, X. G., Zhou, X.-Z., Xie, L., Dunlop, M. W., et al. (2007). Global view of dayside magnetic reconnection with the dawn-dusk IMF orientation: A statistic study for TC-1 and Cluster data. *Geophysical Research Letters*, *34*, L20101. https://doi.org/10.1029/2007GL030336

Raeder, J. (2006). Flux transfer events: Generation mechanism for strong southward IMF. *Annales de Geophysique*, *24*, 381–392.

Russell, C. T., Anderson, B. J., Baumjohann, W., Bromund, K. R., Dearborn, D., Fischer, D., et al. (2016). The magnetospheric multiscale magnetometers. *Space Science Reviews*, *199*(1-4), 189–256 https://doi.org/10.1007/s11214-014-0057-3

Schreier, R., Swisdak, M., Drake, J. F., & Cassak, P. A. (2010). Three-dimensional simulations of the orientation and structure of reconnection X-lines. *Physics of Plasmas*, *17*(11), 110,704.

Sonnerup, B. U. Ö. (1974). The reconnecting magnetosphere. In B. M. McCormas (Ed.), *Magnetospheric physics*, Proceedings of the Advanced Summer Institute, held at Sheffield, UK, 1973, *Astrophysics and Space Science Library* (Vol. 44, p. 23). Dortrecht: Reidel.

Swisdak, M., & Drake, J. F. (2007). Orientation of the reconnection X-line. *Geophysical Research Letters*, *34*, L11106. https://doi.org/10.1029/2007GL029815

Teh, W.-L., & Sonnerup, B. U. O. (2008). First results from ideal 2-D MHD reconstruction: Magnetopause reconnection event seen by Cluster. *Annales de Geophysique*, *26*(9), 2673–2684.

Torbert, R. B., Russell, C. T., Magnes, W., Ergun, R. E., Lindqvist, P. A., LeContel, O., et al. (2016). The FIELDS instrument suite on MMS: Scientific objectives, measurements, and data products. *Space Science Reviews*, *199*(1-4), 105–135. https://doi.org/10.1007/s11214-014-0109-8

Trattner, K. J., Burch, J. L., Ergun, R., Eriksson, S., Fuselier, S. A., Giles, B. L., et al. (2017). The MMS dayside magnetic reconnection locations during phase 1 and their relation to the predictions of the maximum magnetic shear model. *Journal of Geophysical Research: Space Physics*, *122*, 11,991–12,005. https://doi.org/10.1002/2017JA024488

Trattner, K. J., Mulcock, J. S., Petrinec, S. M., & Fuselier, S. A. (2007). Probing the boundary between anti-parallel and component reconnection during southwards interplanetary magnetic field conditions. *Journal of Geophysical Research*, *112*, A08210. https://doi.org/10.1029/2007JA012270

Trattner, K. J., Petrinec, S. M., Fuselier, S. A., & Phan, T. D. (2012). The location of the reconnection line: Testing the maximum magnetic shear model with THEMIS observations. *Journal of Geophysical Research*, *117*, A01201. https://doi.org/10.1029/2011JA016959

Trattner, K. J., Thresher, S., Trenchi, L., Fuselier, S. A., Petrinec, S. M., Peterson, W. K., & Marcucci, M. F. (2017). On the occurrence of magnetic reconnection equatorward of the cusps at the Earth's magnetopause during northward IMF conditions. *Journal of Geophysical Research: Space Physics*, *122*, 605–617. https://doi.org/10.1002/2016JA023398

Trenchi, L., Marcucci, M. F., Pallocchia, G., Consolini, G., Bavassano Cattaneo, M. B., Di Lellis, A. M., et al. (2008). Occurrence of reconnection jets at the dayside magnetopause: Double Star observations. *Journal of Geophysical Research*, *113*, A07S10. https://doi.org/10.1029/2007JA012774

Trenchi, L., Marcucci, M. F., Rème, H., Carr, C. M., & Cao, J. B. (2011). TC-1 observations of a flux rope: Generation by multiple X-line reconnection. *Journal of Geophysical Research*, *116*, A05202. https://doi.org/10.1029/2010JA015986

Tsyganenko, N. A. (1995). Modeling the Earth's magnetospheric magnetic field confined within a realistic magnetopause. *Journal of Geophysical Research*, *100*(A4), 5599–5612. https://doi.org/10.1029/94JA03193

Vines, S. K., Fuselier, S. A., Petrinec, S. M., Trattner, K. J., & Allen, R. C. (2017). Occurrence frequency and location of magnetic islands at the dayside magnetopause. *Journal of Geophysical Research: Space Physics*, *122*, 4138–4155. https://doi.org/10.1002/2016JA023524

Webster, J. M., Ergun, J. L., Reiff, P. H., Daou, A. G., Genestreti, K. J., Graham, D. B., et al. (2018). Magnetospheric Multiscale dayside reconnection electron diffusion region events. *Journal of Geophysical Research: Space Physics*, *123*, 4858–4878. https://doi.org/10.1029/2018JA025245

Young, D. T., Burch, J. L., Gomez, R. G., De Los Santos, A., Miller, G. P., Wilson, P. IV, et al. (2016). Hot Plasma Composition Analyzer for the Magnetospheric Multiscale Mission. *Space Science Reviews*. https://doi.org/10.1007/s11214-014-0119-6